Vol 18 No 3, March 2009
1674-1056/2009/18(03)/1227-04
Chinese Physics B
© 2009 Chin. Phys. Soc.
and IOP Publishing Ltd

Frequency selective surface with better polarization independency for arbitrary incident angle*

Jia Hong-Yan(贾宏燕)[a)b)], Gao Jin-Song(高劲松)[a)], and Feng Xiao-Guo(冯晓国)[b)]

[a)] *Changchun Institute of Optics, Fine Mechanics and Physics, Chinese Academy of Sciences, Changchun* 130033, *China*

[b)] *Graduate University of Chinese Academy of Sciences, Beijing* 100049, *China*

(Received 18 April 2008; revised manuscript received 10 July 2008)

This paper investigates the frequency-selective property of a planar layer consisting of period arrays both theoretically and experimentally for different polarizations at arbitrary incident angle. The novel element is designed by loading the rectangular microstrip element with L-shaped conducting patch at its two ends. Based on the spectral-domain method, the frequency response including angle effect and polarization effect of the frequency selective surface (FSS) structure are analysed and the plots of the frequency versus transmission coefficient are obtained. As a result of the numerical analysis, it is shown that if the source polarization is changed, polarization-independence of previous FSS design can be achieved only for normal incidence, which limits most FSS applications. But in our proposed structure, the better polarization-independency for arbitrary incident angle can be achieved. It is observed that the simulated result comes very close to the experimental result.

Keywords: frequency selective surface (FSS), arbitrary incident angle, polarization independency
PACC: 7300, 7360

1. Introduction

Frequency selective surface (FSS) exhibits frequency filtering properties similar to those of frequency filters in traditional radiofrequency (RF) circuits, which have received immense attention due to their ability to control the propagation of electromagnetic wave.[1−9]

Because of its filtering property, there are two major applications of FSS. One is in reflector antenna systems, where FSS reflectors are used to separate feeds of different bands. The other application is to use FSS as antenna radomes for better control of the transmitted and reflected electromagnetic waves.[10] The proposed FSS design is better polarization-independency for arbitrary incident angle, which makes it attractive for the above mentioned applications in curved FSS.

Several authors have shown that it is possible to achieve polarization independency for FSS structure.[11,12] Recently, Ditti and Das[13] reported computational and experimental results of a FSS made up of rectangular microstrip patches, where only the case of normal incidence was treated. It is worth noting that it is more useful to achieve polarization independency in the case of oblique incidence. The purpose of this work is to describe the results of the spectral-domain analysis on a polarization independent FSS comprised a modified element for arbitrary incidence of plane electromagnetic waves. The modified element is designed by loading the rectangular microstrip element with L-shaped conducting patch at its two ends. Meanwhile, the results of presented FSS are compared with the previous work about FSS made up of rectangular microstrip patches.

2. Design models

Two FSS structures are shown in Figs.1 and 2, respectively.

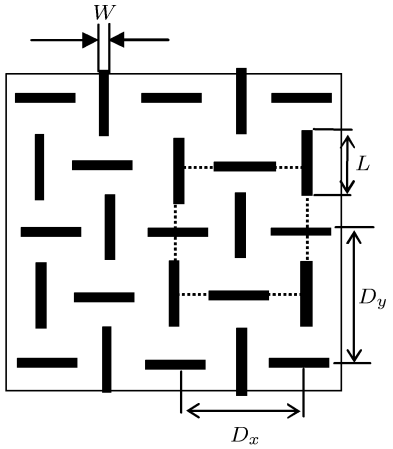


Fig.1. Previous FSS structure.

*Project supported by the National Defense Innovation Foundation of Chinese Academy of Sciences (Grant No CXJJ-149).

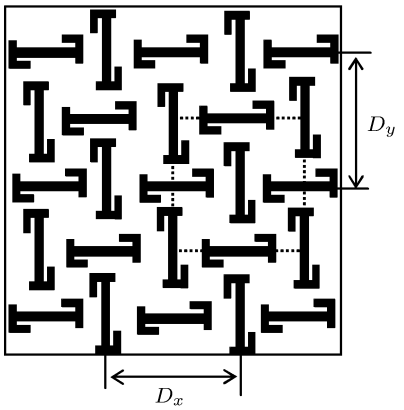


Fig.2. Modified FSS structure.

They are structure (a) which is previous FSS structure designed by Ditti and Das, and structure (b) which is FSS with modified element designed by loading the rectangular microstrip element with L-shaped conducting patch.

For structure (a), the length of each element remains the same, which is chosen to be L=11 mm. Also, the FSS screen has been fabricated on a supporting substrate with dielectric constant of 2.5 and thickness of 0.8 mm. The width of each element is W=1.1 mm, and $D_x = D_y = 22$ mm. For structure (b), the length of the rectangular microstrip is 6 mm, the total length of the L shaped load is 5.2 mm, and $D_x = D_y = 14$ mm. The width of each patch is W=0.8 mm. The parameters of supporting substrate stay the same. The simulated model assumes an infinite periodic array, while for practical implementation, the prototype array has an overall dimension of 500 mm×500 mm.

3. Computational method

The frequency responses of two FSS structures are analysed based on the spectral-domain method.[2]

The solution is obtained by modifying the integral equation corresponding to a single patch element to include the contributions from an array of patches.

The scattered field from a conducting patch on the $x-y$ plane due to an incident plane wave can be calculated from the induced current on the radiating patch. The scattered field at point $\boldsymbol{r}$ due to a source at point $\boldsymbol{r}'$ is

$$\boldsymbol{E}^s = -\mathrm{j}\omega\mu_0\boldsymbol{R} + \frac{1}{\mathrm{j}\omega\varepsilon_0}\nabla(\nabla\cdot\boldsymbol{R}). \tag{1}$$

Where

$$\boldsymbol{R}(\boldsymbol{r}) = \int G(\boldsymbol{r},\boldsymbol{r}')\boldsymbol{J}(\boldsymbol{r}')\mathrm{d}r' = G^*\boldsymbol{J},$$

$$G(\boldsymbol{r},\boldsymbol{r}') = \frac{\mathrm{e}^{-\mathrm{j}k_0|\boldsymbol{r}-\boldsymbol{r}'|}}{4\pi|\boldsymbol{r}-\boldsymbol{r}'|},$$

and G is the Green's function. $\boldsymbol{J}$ is the induced surface current on the conductor.

The electric-field integral equation of spatial domain expression for the patches elements array is obtained as follows:

$$\begin{aligned}
&-\begin{bmatrix} E_x^{\mathrm{i}}(x,y) \\ E_y^{\mathrm{i}}(x,y) \end{bmatrix} \\
=&\frac{2\pi}{\mathrm{j}\omega\varepsilon_0 D_x D_y}\sum_{m=-\infty}^{\infty}\sum_{n=-\infty}^{\infty}\begin{bmatrix} k_0^2-\alpha_m^2 & -\alpha_m\beta_n \\ -\alpha_m\beta_n & k_0^2-\beta_n^2 \end{bmatrix} \\
&\times\tilde{\boldsymbol{G}}(\alpha_m,\beta_n)\begin{bmatrix} \tilde{\boldsymbol{J}}_x(\alpha_m,\beta_n) \\ \tilde{\boldsymbol{J}}_y(\alpha_m,\beta_n) \end{bmatrix}\mathrm{e}^{\mathrm{j}\alpha_m x}\mathrm{e}^{\mathrm{j}\beta_n y},
\end{aligned} \tag{2}$$

where

$$\alpha_{mn} = \frac{2m\pi}{D_x} + k_x^{\mathrm{i}},$$
$$\beta_{mn} = \frac{2n\pi}{D_y\sin\Omega} - \frac{2m\pi}{a}\cot\Omega + k_y^{\mathrm{i}}.$$

We have replaced the convolution and partial derivatives by $G * \boldsymbol{J} \to \tilde{G}\tilde{\boldsymbol{J}}$, $\partial\boldsymbol{R}/\partial x \to \mathrm{j}\alpha\boldsymbol{R}$ and $\partial\boldsymbol{R}/\partial y \to \mathrm{j}\beta\boldsymbol{R}$ in the Fourier domain. And the superscript i corresponds to the incident field. Ω is the skew angle, here, Ω=90°.

For $k_0^2 > \alpha^2+\beta^2$,

$$\tilde{\boldsymbol{G}} = \frac{-\mathrm{j}}{2\sqrt{k_0^2-\alpha^2-\beta^2}}\boldsymbol{I}.$$

Otherwise,

$$\tilde{\boldsymbol{G}} = \frac{1}{2\sqrt{\alpha^2+\beta^2-k_0^2}}\boldsymbol{I},$$

($\boldsymbol{I}$ is an identity tensor).

The elements in dashed rectangular frame are selected as the unit cell for two structures, shown in Figs.1 and 2 respectively, which are discretized to employ rooftop subdomain basis function.

Equation (2) can be solved with the method of moments, which yields the unknown surface current distribution on the patch of a FSS screen. Then we can determine the transmission coefficient.

4. Result and discussion

By using the spectral-domain method, the plots of the frequency versus transmission coefficient are obtained for different polarizations at arbitrary incident angles to illustrate that structure (b) possesses better polarization-independency property for large incident angles than that of the structure (a).

Figure 3 presents the plots of transmission coefficient versus frequency of structure (a). For the normal incidence, this FSS exhibits a good performance. The frequency response of the FSS remains independent of the source polarization, which is in agreement with the result reported in Ref.[11]. But it suffers from an unwanted variation of resonance frequency over a varying polarization for 45° incidence angle. The resonance frequency shift to 10 GHz for TM 45° from 11 GHz for TE 45 °, a large deviation of 1GHz is observed.

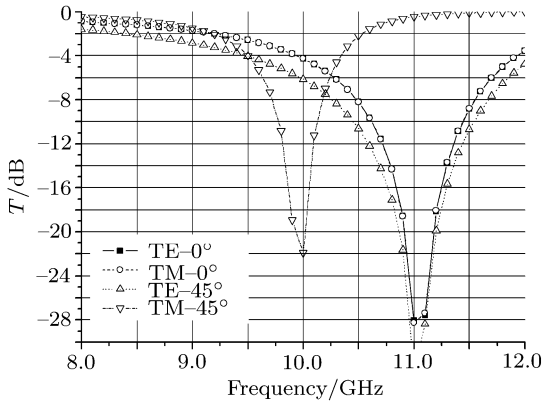


Fig.3. Simulated transmission coefficient T vs frequency of structure (a) for different incidences.

A positive result may expect in the case of structure (b). The computational transmission response (Fig.4) shows that the resonant frequency is 8.5 GHz for the normal incidence and TE 45°, 8.6 GHz for TM 45°. This depicts a relatively stable transmission response at the stop band region for different polarizations at different incident angles, i.e. 0° and 45°.

Some negligible differences occur in the resonance frequency and stop-band width. A comparison of data from Fig.4 demonstrates that the stop-band width is increased for TE incidence, while the width is decreased for TM incidence when the angle changes from 0° to 45°. Meanwhile, the resonance frequency is change insignificantly and only a small deviation of 0.1 GHz is observed. As the angles and polarizations changed, the FSS bandwidth and resonance frequency are relatively stable. This is a remarkable improvement in comparison with structure (a).

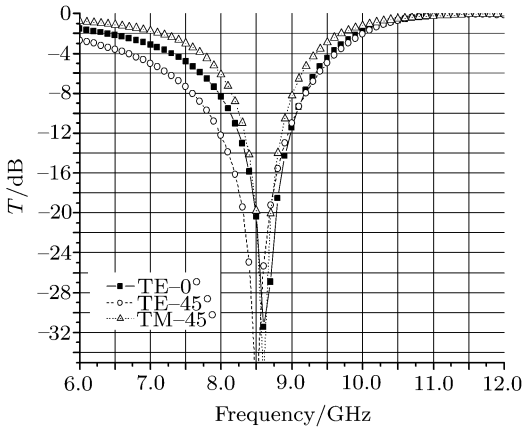


Fig.4. Simulated transmission coefficient T vs frequency of structure (b) for different incidences.

5. Measurement

With film technology and lithography, two FSS samples are made. The transmission coefficient over the frequency range 4–8 GHz and 8–12 GHz is measured for structure (b) in the anechoic chamber. The scanning step is 0.1 GHz. Only 8–12 GHz frequency range is needed for structure (a)

For the normal incidence, the polarization of the incident wave on the FSS can be changed from vertical to horizontal without disturbing the measurement setup by rotating the FSS screen 90° about the axis penetrating through the centre of the structure. However, the method is not workable when the large incident angles are concerned. In this situation, the feedhorn must be rotated 90° to change the polarization of the incident wave.

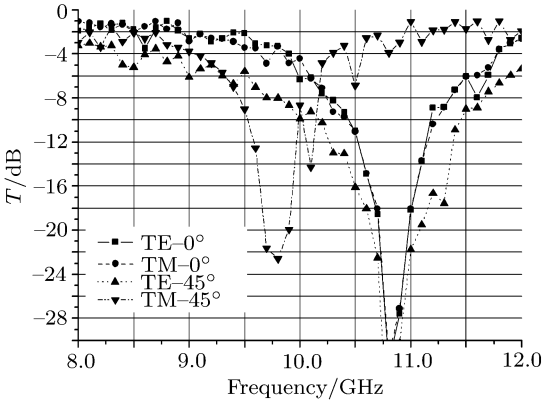


Fig.5. Measured transmission coefficient T vs frequency of structure (a) for different incidences.

The experimental results for both FSS structure are shown in Figs.5 and 6, respectively. The simulated result agrees with the experimental observation to a great extent. The difference occurs in the resonance frequency, where less than 0.5GHz deviation to the lower frequency range is observed. May be this deviation is caused by the error of substrate dielectric parameters.

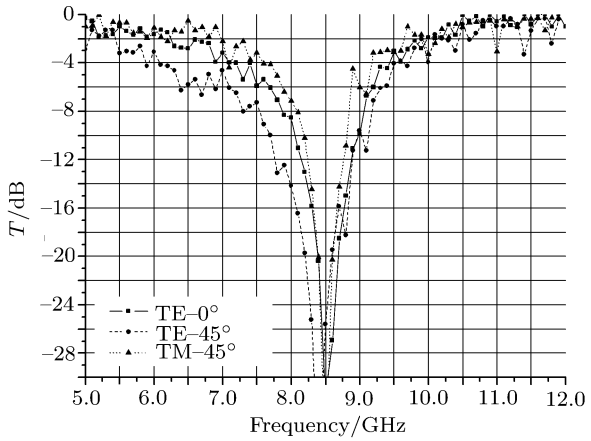


Fig.6. Measured transmission coefficient T vs frequency of structure (b) for different incidences.

6. Conclusion

This work presents a theoretical and experimental study of novel element FSS. The performance of proposed FSS structure remains stable for input waves with different polarizations at arbitrary incident angles. It is observed that the simulated result comes very close to the experimental result. This FSS gives us a new design method for the situation in which the polarization of the source is completely unpredictable and curved FSS application for which arbitrary incident angle must be taken into account.

References

[1] Munk B A 2000 *Frequency Selective Surface: Theory and Design* (New York: Wiley)
[2] Wu T K 1995 *Frequency Selective Surface and Grid Array* (New York: Wiley)
[3] Munk B A 2003 *FSS and Finite Antenna Array* (New York: Wiley)
[4] Li X Q 2006 *Optics and Precision Engineering* **14** 1070
[5] He B 2005 *Optics and Precision Engineering* **13** 599
[6] Lu J, Zhang J and Sun L C 2005 *Optics and Precision Engineering* **13** 219 (in Chinese)
[7] He B and Cong Y L 2006 *Optics and Precision Engineering* **14** 704
[8] Li X Q 2008 *Acta Phys. Sin.* **57** 4082 (in Chinese)
[9] Li X Q 2008 *Acta Phys. Sin.* **57** 4912 (in Chinese)
[10] Pelton E L and Munk B A 1974 *IEEE Trans. Antennas Propagat.* **32** 799
[11] Jia H Y 2007 *Optics and Precision Engineering* **15** 978
[12] Pelton E L and Munk B A 1979 *IEEE Trans. Antennas Propagat.* **AP-27**, 323
[13] Ditti S K and Das S 2005 *Microwave and Optical Technology Letters* **44** 249